Inorg. Chem. **2009**, *48*, 518−526

Very Fast Single-Step Photoinduced Charge Separation in Zinc Porphyrin Bridged to a Gold Porphyrin by a Bisethynyl Quaterthiophene

Jérôme Fortage,[†] Julien Boixel,[†] Errol Blart,[†] Hans Christian Becker,[*,‡] and Fabrice Odobel[*,†]

Université de Nantes, CEISAM, Chimie Et Interdisciplinarité, Synthèse, Analyse, Modélisation, Faculté des Sciences et des Techniques, 2, rue de la Houssinière, BP 92208, 44322 NANTES Cedex 3, France, and CNRS, UMR 6230, Department of Photochemistry and Molecular Science, The Ångström Laboratories, Uppsala University, Regementsvägen 1, 752 37 Uppsala, Sweden

Received April 23, 2008

A new heterometallic dyad composed of a zinc porphyrin linked by bisethynyl quaterthiophene to a gold porphyrin was synthesized according to a stepwise modular approach. The latter dyad and the parent reference compounds (porphyrin-ethynylquaterthiophene) were characterized by electrochemistry, spectroelectrochemistry, and femtosecond transient absorption spectrocopy. We showed that light excitation of the zinc or the gold porphyrin induces a very fast and quantitative charge separation over a distance of 25 Å which occurs through a superexchange mechanism. The lifetime of the charge-separated state is 3.3 ns in toluene and 100 ps in dichloromethane, and it recombines to the ground state in both solvents.

Introduction

Linear multichromophoric arrays for photoinduced charge separation represent extremely important targets, owing to their potential applications for solar energy conversion and optoelectronics.[1−3] We have been particularly interested in the design of electronically coupled arrays to achieve long-range charge separations in a single step with porphyrin derivatives.[4−7] To reach this goal, the attachment of the spacer directly on a meso position of a porphyrin via an ethynyl moiety represents an effective strategy to make effective long-range photoinduced processes.[4,6−8] This strategy contrasts with the usual approach of connecting the spacer on a meso aryl substituent of the porphyrin.[3] The large dihedral angle between the porphyrin macrocycle and the meso aryl group prevents efficient mixing of the electronic wave functions of the linked elements and thereby limits the electronic coupling, whereas the ethynyl linker increases the distance between the porphyrin and the spacer and permits an extensive π-conjugation and therefore electronic communication.[4,6,8,9] In the donor−spacer−acceptor model systems, it has been recognized theoretically and then experimentally that the spacer controls the rate of the forward and backward charge separation between the donor and the

* Authors to whom correspondence should be addressed. Tel.: +46-18-471 3648(H.C.B.), +33 2 51 12 54 29(F.O.). Fax: +46-18-471 6844 (H.C.B.), +33 2 51 12 54 02 (F.O.). E-mail: hcb@fotomol.uu.se (H.C.B.), Fabrice.Odobel@univ-nantes.fr (F.O.).

† Université de Nantes.

‡ Uppsala University.

(1) (a) *Electron Transfer in Chemistry*; Balzani, V.; Piotrowiak, P.; Rodgers, M. A. J.; Mattay, J.; Astruc, D.; Gray, H. B.; Winkler, J.; Fukuzumi, S.; Mallouk, T. E.; Haas, Y.; de Silva, A. P.; Gould, I., Eds.; Wiley-VCH: Weinheim, 2001. (b) *Supramolecular Photochemistry*; Balzani, V.; Scandola, F., Eds; Reidel: Chischester, U. K., 1991.

(2) (a) Gust, D.; Moore, T. A.; Moore, A. L. *Acc. Chem. Res.* **1993**, *26*, 198. (b) Gust, D.; Moore, T. A.; Moore, A. L.; Lee, S. J.; Bittersmann, E.; Luttrull, D. K.; Rehms, A. A.; DeGraziano, J. M.; Ma, X. C.; Gao, F.; Belford, R. E.; Trier, T. T. *Science* **1990**, *248*, 199. (c) Bard, A. J.; Fox, M. A. *Acc. Chem. Res.* **1995**, *28*, 141. (d) Joachim, C.; Gimzewski, J. K.; Aviram, A. *Nature* **2000**, *408*, 541.

(3) Wasielewski, M. R. *Chem. Rev.* **1992**, *92*, 435.

(4) Fortage, J.; Boixel, J.; Blart, E.; Hammarström, L.; Becker, H.-C.; Odobel, F. *Chem.—Eur. J.* **2008**, *14*, 3467.

(5) (a) Blart, E.; Suzenet, F.; Quintard, J.-P.; Odobel, F. *J. Porphyrins Phthalocyanines* **2003**, *7*, 207. (b) Chaignon, F.; Torroba, J.; Blart, E.; Borgström, M.; Hammarström, L.; Odobel, F *New J. Chem.* **2005**, *29*, 1272. (c) Odobel, F.; Suzenet, F.; Blart, E.; Quintard, J.-P. *Org. Lett.* **2000**, *1*, 131.

(6) Monnereau, C.; Gomez, J.; Blart, E.; Odobel, F.; Wallin, S.; Fallberg, A.; Hammarström, L. *Inorg. Chem.* **2005**, *44*, 4806.

(7) Fortage, J.; Goeransson, E.; Blart, E.; Becker, H.-C.; Hammarström, L.; Odobel, F. *Chem. Commun.* **2007**, 4629.

(8) (a) Winters, M. U.; Dahlstedt, E.; Blades, H. E.; Wilson, C. J.; Frampton, M. J.; Anderson, H. L.; Albinsson, B. *J. Am. Chem. Soc.* **2007**, *129*, 4291. (b) Kelley, R. F.; Tauber, M. J.; Wasielewski, M. R. *Angew. Chem., Int. Ed.* **2006**, *45*, 7979. (c) Kelley, R. F.; Tauber, M. J.; Wilson, T. M.; Wasielewski, M. R. *Chem. Commun.* **2007**, 4407.

(9) Odobel, F.; Suresh, S.; Blart, E.; Nicolas, Y.; Quintard, J.-P.; Janvier, P.; Questel, J.-Y. L.; Illien, B.; Rondeau, D.; Richomme, P.; Häupl, T.; Wallin, S.; Hammarström, L. *Chem.—Eur. J.* **2002**, *8*, 3027–3046.

10.1021/ic800727e CCC: $40.75
Published on Web 12/12/2008

acceptor.[1,10,11] Wasielewski and co-workers[12] as well as Guldi and co-workers[13] have recently developed dyads, linked by a long π-conjugated spacer, capable of efficient electron transfer (ET) over very long distances. Oligothiophenes represent an attractive class of π-conjugated molecules that can be used as spacers, or as the photoactive unit in molecular devices for electron transfer, especially for photovoltaic applications.[14] We have previously shown that bisethynyl quaterthiophene was suitable to efficiently mediate energy transfer between a zinc and a free base porphyrin.[9] The linking of a zinc porphyrin to a gold porphyrin is particularly amenable to photoinduced charge separation, as already shown by Sauvage and co-workers,[15,16] Albinsson and co-workers,[17] and Fukuzumi and co-workers.[18,19]

We now report the stepwise preparation and the photophysical properties of a new heterometallic bisporphyrin system composed of a zinc porphyrin as the electron donor and a gold porphyrin as the electron acceptor. This dyad demonstrates the suitability of the bisethynyl quaterthiophene spacer to promote very fast single-step charge separation upon excitation of either porphyrin component.

Experimental Section

Materials and Methods. ^{1}H and ^{13}C NMR spectra were recorded on a Bruker ARX 300 MHz or a Bruker AMX 400 MHz spectrometer. Chemical shifts for ^{1}H NMR spectra are referenced relative to residual protium in the deuterated solvent ($CDCl_3$ δ = 7.26 ppm). High-resolution electro-spray mass spectra were collected in the positive mode on a Micromass MS/MS ZABSpec TOF apparatus equipped with a geometry EBE TOF. The samples were injected into a mixture of 9:1 $CHCl_3$/MeOH. Electron-impact mass spectra were recorded on a HP 5989A spectrometer. Matrix-assisted laser desorption mass spectrometry analyses were performed on Bruker biflex III MALDI-TOF spectrometer using cyano 4-hydroxycinnamic acid (CHCA) or dithranol as the matrix. The instrument is equipped with a nitrogen laser emitting at 337 nm, a 2-GHz sampling rate digitizer, a pulsed ion extraction source, and a reflectron.

Thin-layer chromatography (TLC) was performed on aluminum sheets precoated with Merck 5735 Kieselgel 60F254. Column chromatography was carried out either with Merck 5735 Kieselgel 60F (0.040−0.063 mm mesh) or with SDS neutral alumina (0.05−0.2 mm mesh). Air-sensitive reactions were carried out under argon in dry solvents and glassware. Chemicals were purchased from Aldrich or Acros and used as received. The solvents for the reactions were distillated prior to use following the standard purification procedures. The compounds 3,3‴-dioctyl-[2,2′;5′,2″;5″,2‴] quaterthiophene (**1**),[20] zinc(II)-5,15-bis-(3,5-diterbutyl phenyl)-10-phenyl-20-iodoporphyrin (**7**),[4] and the mixture of gold(III)-5,15-bis-(3,5-diterbutylphenyl)-10-phenyl-20-bromoporphyrin and gold(III)-5,15-bis-(3,5-diterbutylphenyl)-10-phenyl-20-chloroporphyrin (**8**)[4] were prepared according to literature methods.

Electrochemistry and Spectroelectrochemistry. The electrochemical measurements were performed with a potentiostat-galvanostat MacLab model ML160 controlled by resident software (Echem v1.5.2 for Windows) using a conventional single-compartment three-electrode cell. The working electrode was a platinum disk of 4 mm^2 area. The auxiliary electrode was a Pt wire, and the reference electrode was a saturated potassium chloride calomel electrode (SCE). The supporting electrolyte was 0.15 M Bu_4NPF_6 in dichloromethane, and the solutions were purged with argon before the measurements. All potentials are quoted relative to SCE. In all of the experiments, the scan rate was 100 mV/s for the cyclic voltammetry and 15 Hz for pulse voltammetry. Spectroelectrochemical spectra were recorded in a thin quartz UV−visible cell (0.5 mm) equipped with a reference electrode (SCE) and a platinum wire as the counter electrode. The working electrode was a platinum grid inserted within the quartz cell, and the other conditions were the same as those for the cyclic voltammetry.

Spectroscopy. UV−visible absorption spectra were recorded on a UV-2401PC Shimadzu spectrophotometer. Fluorescence spectra

(10) (a) Benniston, A. C.; Harriman, A. *Chem. Soc. Rev.* **2006**, *35*, 169. (b) Holten, D.; Bocian, D. F.; Lindsey, J. S. *Acc. Chem. Res.* **2002**, *35*, 57. (c) Paddon-Row, M. N. *Acc. Chem. Res.* **1994**, *27*, 18.

(11) Adams, D. M.; Brus, L.; Chidsey, C. E. D.; Creager, S.; Creutz, C.; Kagan, C. R.; Kamat, P. V.; Lieberman, M.; Lindsay, S.; Marcus, R. A.; Metzger, R. M.; Michel-Beyerle, M. E.; Miller, J. R.; Newton, M. D.; Rolison, D. R.; Sankey, O.; Schanze, K. S.; Yardley, J.; Zhu, X. *J. Phys. Chem. B* **2003**, *107*, 6668.

(12) (a) Davis, W. B.; Ratner, M. A.; Wasielewski, M. R. *J. Am. Chem. Soc.* **2001**, *123*, 7877. (b) Davis, W. B.; Svec, W. A.; Ratner, M. A.; Wasielewski, M. R. *Nature* **1998**, *396*, 60. (c) Hayes, R. T.; Wasielewski, M. R.; Gosztola, D. *J. Am. Chem. Soc.* **2000**, *122*, 5563.

(13) (a) Giacalone, F.; Segura, J. L.; Martin, N.; Ramey, J.; Guldi, D. M. *Chem.—Eur. J.* **2005**, *11*, 4819. (b) Vail, S. A.; Krawczuk, P. J.; Guldi, D. M.; Palkar, A.; Echegoyen, L.; Tome, J. P. C.; Fazio, M. A.; Schuster, D. I. *Chem.—Eur. J.* **2005**, *11*, 3375. (c) De la Torre, G.; Giacalone, F.; Segura, J. L.; Martin, N.; Guldi, D. M. *Chem.—Eur. J.* **2005**, *11*, 1267. (d) Giacalone, F.; Segura, J. L.; Martin, N.; Guldi, D. M. *J. Am. Chem. Soc.* **2004**, *126*, 5340. (e) Atienza-Castellanos, C.; Wielopolski, M.; Guldi, D. M.; van der Pol, C.; Bryce, M. R.; Filippone, S.; Martin, N. *Chem. Commun.* **2007**, 5164.

(14) (a) Nakamura, T.; Kanato, H.; Araki, Y.; Ito, O.; Takimiya, K.; Otsubo, T.; Aso, Y. *J. Phys. Chem. A* **2006**, *110*, 3471. (b) Otsubo, T.; Aso, Y.; Takimiya, K. *Pure Appl. Chem.* **2005**, *77*, 2003. (c) Nakamura, T.; Ikemoto, J.; Fujitsuka, M.; Araki, Y.; Ito, O.; Takimiya, K.; Aso, Y.; Otsubo, T. *J. Phys. Chem. B* **2005**, *109*, 14365. (d) Kanato, H.; Takimiya, K.; Otsubo, T.; Aso, Y.; Nakamura, T.; Araki, Y.; Ito, O. *J. Org. Chem.* **2004**, *69*, 7183. (e) Nakamura, T.; Fujitsuka, M.; Araki, Y.; Ito, O.; Ikemoto, J.; Takimiya, K.; Aso, Y.; Otsubo, T. *J. Phys. Chem. B* **2004**, *108*, 10700. (f) Otsubo, T.; Aso, Y.; Takimiya, K. *J. Mater. Chem.* **2002**, *12*, 2565. (g) Ikemoto, J.; Takimiya, K.; Aso, Y.; Otsubo, T.; Fujitsuka, M.; Ito, O. *Org. Lett.* **2002**, *4*, 309. (h) Oike, T.; Kurata, T.; Takimiya, K.; Otsubo, T.; Aso, Y.; Zhang, H.; Araki, Y.; Ito, O. *J. Am. Chem. Soc.* **2005**, *127*, 15372. (i) Oswald, F.; Islam, D. M. S.; Araki, Y.; Troiani, V.; Caballero, R.; de la Cruz, P.; Ito, O.; Langa, F. *Chem. Commun.* **2007**, 4498.

(15) (a) Brun, A. M.; Atherton, S. J.; Harriman, A.; Heitz, V.; Sauvage, J. P. *J. Am. Chem. Soc.* **1992**, *114*, 4632. (b) Chambron, J. C.; Harriman, A.; Heitz, V.; Sauvage, J. P. *J. Am. Chem. Soc.* **1993**, *115*, 6109.

(16) (a) Brun, A. M.; Harriman, A.; Heitz, V.; Sauvage, J.-P. *J. Am* **1991**, *113*, 8657–8663. (b) Harriman, A.; Heitz, V.; Chambron, J. C.; Sauvage, J. P. *Coord. Chem. Rev.* **1994**, *132*, 229. (c) Harriman, A.; Heitz, V.; Sauvage, J. P. *J. Phys. Chem.* **1993**, *97*, 5940.

(17) (a) Andréasson, J.; Kodis, G.; Ljungdahl, T.; Moore, A. L.; Moore, T. A.; Gust, D.; Mårtensson, J.; Albinsson, B. *J. Phys. Chem. A* **2003**, *107*, 8825. (b) Winters, M. U.; Pettersson, K.; M, J. *Chem.—Eur. J.* **2005**, 11. (c) Pettersson, K.; Wiberg, J.; Ljungdahl, T.; Mårtensson, J.; Albinsson, B. *J. Phys. Chem. A* **2006**, *110*, 319. (d) Kilsa, K.; Kajanus, J.; Macpherson, A. N.; Mårtensson, J.; Albinsson, B. *J. Am. Chem. Soc.* **2001**, *123*, 3069. (e) Andreasson, J.; Kodis, G.; Ljungdahl, T.; Moore, A. L.; Moore, T. A.; Gust, D.; Mårtensson, J.; Albinsson, B. *J. Phys. Chem. A* **2003**, *107*, 8825. (f) Wiberg, J.; Guo, L.; Pettersson, K.; Nilsson, D.; Ljungdahl, T.; Mårtensson, J.; Albinsson, B. *J. Am. Chem. Soc.* **2007**, *129*, 155. (g) Eng, M. P.; Albinsson, B. *Angew. Chem., Int. Ed.* **2006**, *45*, 5626.

(18) Fukuzumi, S.; Ohkubo, K. E.; Ou, Z. P.; Shao, J. G.; Kadish, K. M.; Hutchison, J. A.; Ghiggino, K. P.; Sintic, P. J.; Crossley, M. J. *J. Am. Chem. Soc.* **2003**, *125*, 14984.

(19) Ohkubo, K.; Sintic, P. J.; Tkachenko, N. V.; Lemmetyinen, H. E. W.; Ou, Z.; Shao, J.; Kadish, K. M.; Crossley, M. J.; Fukuzumi, S. *Chem. Phys.* **2006**, *326*, 3.

(20) Nakanishi, H.; Sumi, N.; Aso, Y.; Otsubo, T. *J. Org. Chem.* **1998**, *63*, 8632.

were recorded on a SPEX Fluoromax fluorimeter and were corrected for the wavelength-dependent response of the detector system (Hamamatsu R928).

Time-correlated single-photon counting (fwhm ≈ 80 ps) was performed with a Hamamatsu MCP as the detector. Excitation was done with 400 nm, 120 fs pulses from a Coherent RegA Ti:sapphire amplifier.

Transient absorption was performed using a previously described system.[21] Briefly, the output (80 fs, 800 nm) from a Coherent Legend-HE amplifier was used to pump an optical parametric amplifier (TOPAS, Light Conversion) to produce 620 nm light (for ZnP excitation) or 690 nm light (for AuP excitation). Pump intensities were kept below 500 nJ/pulse to avoid nonlinear effects and to minimize sample degradation. Probe light, generated on a CaF_2 plate from a fraction of the 800 nm output, was split into signal and reference beams and detected in a 512-pixel-wide diode array (Pascher Instruments, Lund, Sweden). Data were averaged with a total of 5000−10 000 measurements per time point. The angle between the polarization of the pump and probe was kept at 55°. The sample cell was continously moved up and down to avoid photobleaching and accumulation of the photoproducts. An analysis of transient absorption data was done using the Igor Pro software package (Wavemetrics Inc., Lake Oswego, OR) by iterative reconvolution with a Gaussian response function. The time resolution was, in all cases, better than 300 fs, and the fits were robust with respect to varying initial guesses.

Experimental Procedures for the Synthesis of the Compounds. 5-Bromo-3,3‴-dioctyl-[2,2′;5′,2″;5″,2‴]quaterthiophene (**2**) and 3,3‴-dioctyl-[2,2′;5′,2″;5″,2‴]quaterthiophene (**1**; 240 mg, 0.4 mmol) were dissolved in degassed CS_2 (20 mL) in a three-necked flask. The mixture was cooled to −20 °C, and a solution of NBS (61 mg, 0.34 mmol dissolved in 10 mL of $CHCl_3$) was added dropwise under an argon atmosphere for 1 h. The mixture was stirred at this temperature for half an hour and then brought to 0 °C and stirred for another 30 min.

The mixture was diluted with CH_2Cl_2, and the organic phase was washed with an aqueous saturated solution of ammonium chloride, then with water. The organic phase was dried over $MgSO_4$, and the solvents were evaporated to dryness. The residue was purified by column chromatography over flash silica (petroleum ether) to afford **2** as a yellow oil (164 mg, 65%). ^{1}H NMR (300 MHz, $CDCl_3$, 25 °C): δ 0.87 (m, 6H), 1.31 (m, 20H), 1.58 (m, 4H), 2.71 (t, ^3J = 7.8 Hz, 2H), 2.77 (t, ^3J = 7.8 Hz, 2H), 6.90 (s, 1H), 6.94 (d, ^3J = 5.2 Hz), 6.96 (d, ^3J = 4.2 Hz, 1H), 7.02 (d, ^3J = 3.8 Hz, 1H), 7.11 (d, ^3J = 4.2 Hz), 7.12 (d, ^3J = 3.8 Hz), 7.18 (d, ^3J = 5.2 Hz, 1H). ^{13}C NMR (75 MHz, $CDCl_3$, 25 °C): δ 14.1, 22.7, 29.3, 29.4, 29.5, 30.5, 30.7, 31.9, 110.6, 123.8, 123.9, 124.0, 126.5, 127.0, 127.8, 130.1, 131.8, 132.7, 133.8, 135.6, 136.5, 137.4, 140.0, 140.5. MS (EI), *m*/*z* calcd for $C_{32}H_{41}BrS_4$: 633.8. Found: 634 (83) $[M]^+$, 554 (55), 368 (100).

5-(Triisopropylsilyl)ethynyl-3,3‴-dioctyl-[2,2′;5′,2″;5″,2‴]quaterthiophene, 3. Bromo quaterthiophene **2** (110 mg, 0.17 mmol), triisopropylsilylacetylene (0.23 mL, 1.0 mmol), $Pd_2dba_3 \cdot CHCl_3$ (5 mg, 0.0048 mmol), PPh_3 (10 mg, 0.038 mmol), CuI (4 mg, 0.021 mmol), and diisopropylamine (0.07 mL) were dissolved in triethylamine (15 mL). The solution was purged with argon through three freeze−pump−thaw cycles and was heated at 70 °C overnight. The reaction mixture was quenched with water, and dichloromethane was added. The resulting organic phase was washed with water and dried over $MgSO_4$. The solvents were removed, and the crude product was purified by column chromatography over flash silica gel (petroleum ether) to afford **3** as a yellow oil (114 mg, 91%). ^{1}H NMR (300 MHz, $CDCl_3$, 25 °C): δ 0.87 (m, 6H), 1.12 (s, 21H), 1.27 (m, 20H), 1.63 (m, 4H), 2.69−2.80 (m, 4H), 6.92 (d, ^3J = 5.1 Hz, 1H), 7.01 (d, ^3J = 3.6 Hz, 2H), 7.06 (s, 1H), 7.10−7.12 (dd, ^3J = 3.6 Hz, ^3J = 3.6 Hz, 2H), 7.17 (d, ^3J = 5.1 Hz, 1H). ^{13}C NMR (75 MHz, $CDCl_3$, 25 °C): δ 11.3, 14.1, 18.7, 22.7, 29.2, 29.4, 30.5, 30.7, 31.9, 99.29, 123.9, 126.5, 126.8, 130.1, 131.9, 135.3, 136.5, 139.4, 139.9. MS (EI), *m*/*z* calcd for $C_{43}H_{62}S_4Si$: 734.35. Found: 734 (100) $[M]^+$, 649 (21), 554 (23), 318 (99), 268 (38), 212 (34), 45 (93).

5-(Triisopropylsilyl)ethynyl-5‴-iodo-3,3‴-dioctyl-[2,2′;5′,2″;5″,2‴]quaterthiophene, 4. Triisopropylsilyl)ethynyl quaterthiophene **3** (220 mg, 0.3 mmol), I_2 (84 mg, 0.32 mmol), and bis(trifluoroacetoxy)iodobenzene (168 mg, 0.39 mmol) were mixed in $CHCl_3$ (35 mL) and stirred at room temperature overnight. The reaction mixture was quenched with water, diluted with dichloromethane, and washed with water. The organic phase was dried over $MgSO_4$, and the solvents were rotary evaporated. The residue was purified by column chromatography over flash silica gel (petroleum ether) to afford **4** as a yellow oil (171 mg, 89%). ^{1}H NMR (300 MHz, $CDCl_3$, 25 °C): δ 0.87 (m, 6H), 1.12 (s, 21H), 1.27 (m, 20H), 1.58−1.65 (m, 4H), 2.69−2.74 (m, 4H), 6.95 (d, ^3J = 3.6 Hz, 1H), 7.01 (d, ^3J = 3.6 Hz, 1H), 7.06 (s, 1H), 7.07 (s, 1H), 7.10−7.11 (dd, ^3J = 3.6 Hz, ^3J = 3.6 Hz, 2H). ^{13}C NMR (75 MHz, $CDCl_3$, 25 °C): δ 11.3, 14.1, 18.7, 22.7, 28.9, 29.2, 29.4, 30.4, 30.6, 31.9, 71.9, 96.6, 99.3, 121.4, 124.0, 124.1, 126.8, 127.0, 131.8, 134.0, 134.6, 135.4, 136.2, 136.9, 137.1, 139.5, 139.8, 141.7. MS (EI), *m*/*z* calcd for $C_{43}H_{61}IS_4Si$: 861.2. Found: 861 (33) $[M]^+$, 735 (25), 380 (100), 59 (50), 41 (69).

5-(Triisopropylsilyl)ethynyl-5‴-(trimethylsilyl)ethynyl-3,3‴-dioctyl-[2,2′;5′,2″;5″,2‴]quaterthiophene, 5. Iodo quaterthiophene **4** (171 mg, 0.2 mmol), trimethylsilylacetylene (85 μL, 0.6 mmol), $Pd_2dba_3 \cdot CHCl_3$ (21 mg, 0.02 mmol), PPh_3 (42 mg, 0.16 mmol), CuI (17 mg, 0.09 mmol), and diisopropylamine (84 μL) were dissolved in triethylamine (25 mL). The solution was purged with argon through three freeze−pump−thaw cycles and was heated at 70 °C overnight. The reaction mixture was quenched with water, extracted with dichloromethane, and washed with water. The organic phase was dried over $MgSO_4$, and the solvents were removed. The product was purified by column chromatography over silica gel (petroleum ether), to yield **5** as a yellow fluorescent oil (129 mg, 79%). ^{1}H NMR (300 MHz, $CDCl_3$, 25 °C): δ 0.24 (s, 9H, TMS), 0.87 (m, 6H), 1.12 (s, 21H), 1.27 (m, 20H), 1.62 (m, 4H), 2.69−2.74 (m, 4H), 7.02−7.03 (m, 2H), 7.06 (s, 1H), 7.07 (s, 1H), 7.11−7.13 (m, 2H). ^{13}C NMR (75 MHz, $CDCl_3$, 25 °C): δ 0.0, 11.4, 14.2, 18.8, 22.8, 29.4, 29.5, 30.59, 32.02, 121.0, 121.6, 124.2, 127.1, 134.8, 135.5, 135.8, 137.0, 139.6. UV−vis (CH_2Cl_2): λ/ε (nm/$\times 10^4$ M^{-1} cm^{-1}): 256 (0.86), 289 (0.58), 404 (2.06). MALDI-TOF, *m*/*z* calcd for $C_{48}H_{70}S_4Si_2$: 830.39 $[M]^+$. Found: 830.62 $[M]^+$.

5-(Triisopropylsilyl)ethynyl-5‴-ethynyl-3,3‴-dioctyl-[2,2′;5′,2″;5″,2‴]quaterthiophene, 6. Quaterthiophene **5** (127 mg, 0.15 mmol) and K_2CO_3 (211 mg, 1.53 mmol) were dissolved in dichloromethane (2 mL) and methanol (4 mL). The solution was stirred at room temperature for 3 h. Water was added, and the mixture was extracted with dichloromethane. The organic phase was dried over $MgSO_4$, and the solvents was removed under a vacuum, affording **6** as a yellow oil (116 mg, 100%). ^{1}H NMR (300 MHz, $CDCl_3$, 25 °C): δ 0.88 (m, 6H), 1.14 (s, 21H), 1.28 (m, 20H), 1.59−1.66 (m, 4H), 2.70−2.75 (m, 4H), 3.39 (s, 1H), 7.02−7.04 (m, 2H), 7.07 (s, 1H), 7.11 (s, 1H), 7.11−7.13 (m, 2H). ^{13}C NMR (300 MHz, $CDCl_3$, 25 °C): δ 10.3, 13.1, 17.6, 21.6, 28.2,

(21) Chaignon, F.; Torroba, J.; Blart, E.; Borgström, M.; Hammarström, L.; Odobel, F. *New J. Chem.* **2005**, *29*, 1272.

28.4, 29.4, 30.9, 81.1, 95.6, 98.2, 118.7, 120.4, 123.0, 123.1, 125.8, 126.0, 130.8, 131.4, 133.2, 133.6, 134.3, 135.0, 135.8, 136.2, 138.5. MALDI-TOF, *m/z* calcd for $C_{45}H_{62}S_4Si$: 758.35 $[M]^+$. Found: 758.64 $[M]^+$.

Compound 9. Quaterthiophene **6** (85 mg, 0.11 mmol), the zinc iodoporphyrin **7** (99 mg, 0.10 mmol), $Pd_2dba_3 \cdot CHCl_3$ (24 mg, 0.023 mmol), and $AsPh_3$ (29 mg, 0.093 mmol) were dissolved in dry Et_3N (6 mL) and dry toluene (25 mL). The solution was purged with argon through three freeze−pump−thaw cycles and was heated at 60 °C for 17 h. The solvents were removed, and the product was purified by column chromatography over flash silica (elution with an 8:2 mixture of petroleum ether/CH_2Cl_2) to afford **9** as a green solid (50 mg, 30%). ^{1}H NMR (300 MHz, $CDCl_3$, 25 °C): δ 0.92 (m, 6H), 1.17 (m, 21H), 1.33 (m, 20H), 1.58 (m, 36H), 1.6−1.8 (m, 4H), 2.71−2.77 (m, 4H), 7.03−7.04 (m, 2H), 7.11−7.13 (m, 2H), 7.20−7.23 (m, 2H), 7.29−7.33 (m, 2H), 7.73−7.77 (m, 3H), 7.85 (m, 2H), 8.13 (m, 4H), 8.18−8.21 (m, 2H), 8.87−8.95 (m, 4H), 9.08−9.10 (m, 2H), 9.77−9.79 (m, 2H). UV−vis (CH_2Cl_2), λ/ε (nm/$\times 10^4$ M^{-1} cm^{-1}): 314 (2.23), 379 (3.23), 440 (16.4), 449 (17.8), 560 (1.33), 630 (3.93). MALDI-TOF, *m/z* calcd for $C_{99}H_{116}N_4S_4SiZn$: 1582.7 $[M]^+$. Found: 1582.8 $[M]^+$.

Compound 10. The compound **9** (40 mg, 0.025 mmol) was dissolved in THF (2.2 mL), and Bu_4NF (60 μL, 1 M in THF) was added. The solution was stirred at room temperature for 1.5 h. The THF was removed, and CH_2Cl_2 was added. The organic phase was washed with water, dried over $MgSO_4$, and evaporated to dryness to afford **10** as a green solid (36 mg, 100%). ^{1}H NMR (300 MHz, $CDCl_3$, 25 °C): δ 0.90 (m, 6H), 1.25 (m, 20 H), 1.55 (m, 36H), 1.62−1.70 (m, 2H), 1.77−1.82 (m, 2H), 2.72−2.76 (m, 2H), 2.85−2.90 (m, 2H), 3.40 (s, 1H), 6.98 (s, 1H), 7.06 (m, 1H), 7.12 (s, 1H), 7.15−7.20 (m, 2H), 7.49 (s, 1H), 7.71−7.73 (m, 3H), 7.80 (m, 2H), 8.08 (m, 4H), 8.17−8.19 (m, 2H), 8.83−8.87 (m, 4H), 9.03−9.04 (m, 2H), 9.74 (m, 2H). MALDI-TOF, *m/z* calcd for $C_{90}H_{96}S_4Zn$: 1426.58 $[M]^+$. Found: 1426.40 $[M]^+$.

Compound 12. The quaterthiophene **6** (38 mg, 0.05 mmol), the equimolar mixture of gold bromo and chloro porphyrins **8** (39 mg, 0.033 mmol), Pd(dppf)Cl_2 (5 mg, 0.007 mmol), and CuI (1 mg, 0.007 mmol) were dissolved in dry Et_3N (0.5 mL) and dry DMF (3.1 mL). The solution was purged with argon through three freeze−pump−thaw cycles and was heated at 45 °C for 20 h. CH_2Cl_2 was added, and the organic phase was washed with water and dried over $MgSO_4$. The solvents were removed, and the residue was purified by column chromatography over flash silica (CH_2Cl_2) to afford **12** as a green solid (17 mg, 28%). ^{1}H NMR (300 MHz, $CDCl_3$, 25 °C): δ 0.89 (m, 6H), 1.14 (m, 21H), 1.25 (m, 20H), 1.56 (m, 36H), 1.7−1.8 (m, 4H), 2.68−2.73 (m, 4H), 7.001−7.024 (m, 1H), 7.07 (s, 1H), 7.12 −7.14 (m, 1H), 7.14 −7.19 (m, 2H), 7.67 (s, 1H), 7.83−7.88 (m, 3H), 7.94 (m, 2H), 8.09 (m, 4H), 8.19−8.21 (m, 2H), 9.18−9.24 (m, 4H), 9.38−9.40 (m, 2H), 10.06−10.08 (m, 2H). UV−vis (CH_2Cl_2), λ/ε (nm/$\times 10^4$ M^{-1} cm^{-1}): 422 (4.77), 524 (1.44), 624 (1.44). MALDI-TOF, *m/z* calcd for $C_{99}H_{116}AuN_4S_4Si$: 1713.75 $[M]^+$. Found: 1713.20 $[M]^+$.

Dyad 11. Compound **10** (36 mg, 0.025 mmol), the equimolar mixture of gold bromo and chloro porphyrins **8** (20 mg, 0.017 mmol), Pd(dppf)Cl_2 (2.5 mg, 0.003 mmol), and CuI (1 mg, 0.003 mmol) were dissolved in dry Et_3N (0.75 mL) and dry DMF (3.2 mL). The solution was purged with argon through three freeze−pump−thaw cycles and was heated at 45 °C for 20 h. CH_2Cl_2 was added, and the organic phase was washed with water and dried over $MgSO_4$. The solvents were evaporated, and the residue was purified over preparative TLC (98:2 CH_2Cl_2/MeOH) to afford the dyad **11** as a green solid (21 mg, 50%). ^{1}H NMR (300 MHz, $CDCl_3$, 25 °C): δ 0.90 (m, 6H), 1.25 (m, 20 H), 1.55 (m, 72H), 1.62−1.71 (m, 2H), 1.79−1.82 (m, 2H), 2.52 (m, 2H), 3.12 (m, 2H), 6.98 (s, 1H), 7.10 (m, 1H), 7.12 (s, 1H), 7.15−7.20 (m, 2H), 7.49 (s, 1H), 7.60−7.80 (m, 3H), 7.80−8.00 (m, 5H, 2H), 8.03 (m, 2H), 8.05 (m, 4H), 8.19 (m, 4H), 8.37 (m, 2H), 8.48 (m, 2H), 8.70−8.9 (m, 8H), 9.04 (m, 2H), 9.42 (m, 4H), 10.03 (m, 2H). UV−vis (CH_2Cl_2), λ/ε (nm/$\times 10^4$ M^{-1} cm^{-1}): 305 (2.87), 427 (17.1), 1.59 (447), 574 (1.74), 630 (4.31). MALDI-TOF, *m/z* calcd for $C_{144}H_{150}AuN_8S_4Zn$: 2379.98 $[M]^+$. Found: 2380.00 $[M]^+$.

Scheme 1. Synthesis of the Unsymmetrical Quaterthiophene Spacer **6**[a]

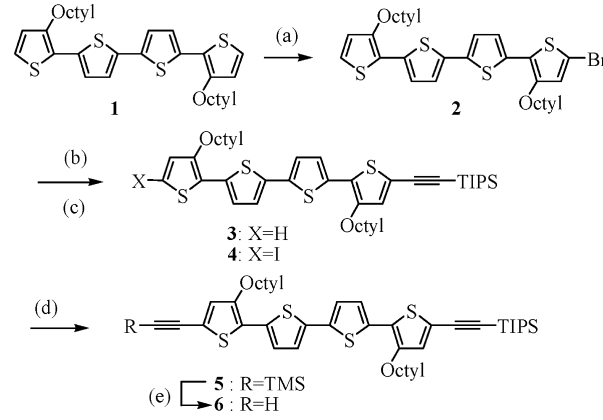

[a] Reagents and conditions: (a) NBS, CS_2, −20°C (65%). (b) HC_2TIPS, CuI, Pd_2dba_3-$CHCl_3$, PPh_3, iPr_2NH, Et_3N (91%). (c) $(CF_3CO_2)_2PhI$, I_2, CCl_4, RT, (89%). (d) HC_2TMS, CuI, Pd_2dba_3-$CHCl_3$, PPh_3, iPr_2NH, Et_3N, 70°C (82%). (e) K_2CO_3, CH_2Cl_2, MeOH, RT (100%).

Results

Synthesis. The preparation of dyad **11** calls for the synthesis of the bisethynyl quaterthiophene spacer **6**, which is illustrated in Scheme 1. The known dioctyl quaterthiophene[22] was initially monobrominated with NBS in a cold mixture of CS_2/DMF in 65% yield.[23] The tris(isopropyl)silylacetylene group was first introduced according to a Sonogashira cross-coupling reaction to give **3**. It was subsequently iodinated with a mixture of iodine/bis(trifluoroacetoxy)iodobenzene in 89% yield.[24] Finally, **4** was subjected to a second Sonogashira cross-coupling reaction, affording **5** with an 82% yield. The trimethylsilyl protecting group was then cleaved with potassium carbonate in a quantitative yield.

The synthesis of dyad **11** is illustrated in Scheme 2. Preparation of the porphyrin building blocks **7** and **8** has been reported elsewhere.[4] Zinc iodo porphyrin **7** was assembled with spacer **6** using a copper-free Sonogashira cross-coupling reaction reported by Lindsey and co-workers.[25] The deprotection of the triisopropylsilyl group was carried out with tetrabutylammonium fluoride, and the resulting acetylenic derivatives were subjected to the final Sonogashira cross-coupling reaction with the mixture of halogeno gold porphyrin **8**. As described previously,[4] we found that the Pd(dppf)Cl_2 catalyst (dppf = diphenylphos-

(22) Nakanishi, H.; Sumi, N.; Aso, Y.; Otsubo, T. *J. Org. Chem.* **1998**, *63*, 8632.
(23) Bäuerle, P.; Würthner, F.; Götz, G.; Effenberger, F. *Synthesis* **1993**, *1993*, 1099.
(24) D'Auria, M.; Mauriello, G. *Tetrahedron Lett.* **1995**, *36*, 4883.
(25) Wagner, R. W.; Johnson, T. E.; Li, F.; Lindsey, J. S. *J. Org. Chem.* **1995**, *60*, 5266.

Scheme 2. Preparation of Dyad **11**[a]

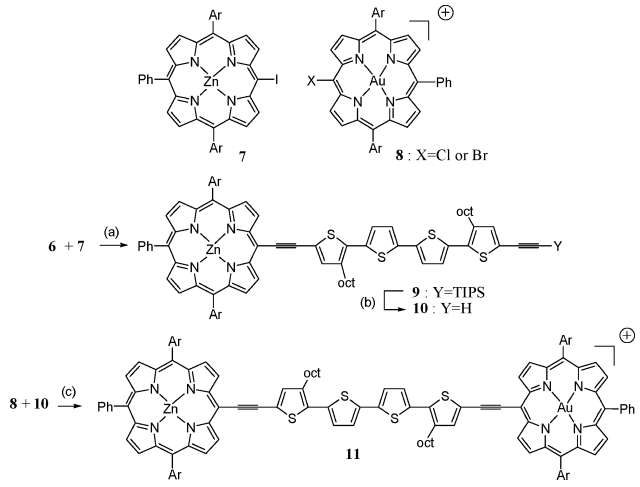

[a] Reagents and conditions: (a) $AsPh_3$, $Pd_2(dba)_3 \cdot CHCl_3$, toluene, Et_3N, 60°C (30%). (b) Bu_4NF, THF, r.t. (100%). (c) **8**, CuI, $Pd(dppf)Cl_2$, Et_3N, DMF, 40−60°C (50%).

Scheme 3. Photophysical Behavior of Dyad **11**

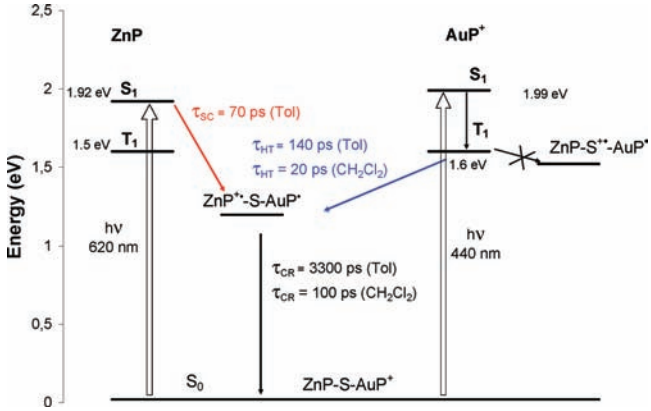

phoferrocene) with copper iodide in a mixture of triethylamine and dimethylformamide proved to be suitable for this coupling, forming dyad **11** with a 50% yield (Scheme 2).[26]

The reference gold prophyrin **12** was also prepared following a Sonogashira cross-coupling reaction between the gold porphyrin **8** and spacer **6** using $Pd(dppf)Cl_2$−CuI as a catalytic system (Figure 1).

Electronic Absorption Spectra. The spectrum of **11** differs significantly from that of a regular tetraaryl zinc or gold porphyrin (Figure S1, Supporting Information). The UV−vis absorption spectrum of dyad **11** along with its components is shown in Figure 2. As observed previously in ethynyl substituted porphyrins, the spectrum of **11** shows a bathochromic shift of all of the visible absorption transitions, a broadening of the Soret band, and an inversion of the intensities of the Q bands (Figure 2).[4,9] These features

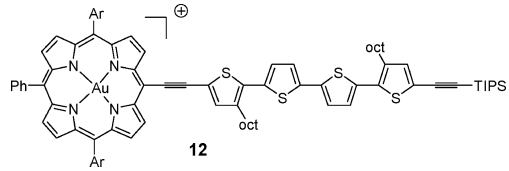

Figure 1. Structure of the reference compound **12**.

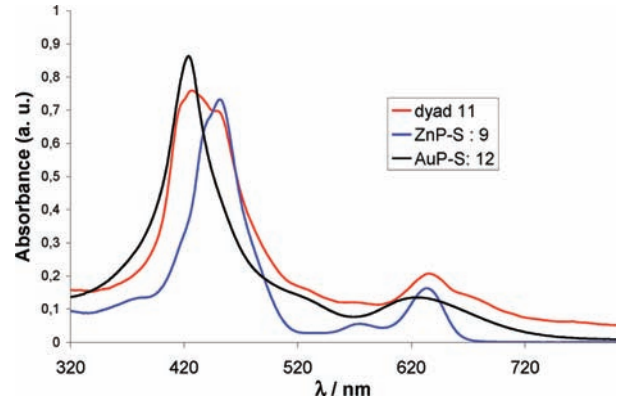

Figure 2. UV−vis absorption spectra of **11** along with those of the reference porphyrins **9** and **12**. The spectra were recorded in dichloromethane.

Table 1. UV−Vis Absorption Data of the Compounds Recorded in Dichloromethane[a]

compound	$\lambda_{max}/\varepsilon$ (nm/M^{-1} cm^{-1})
5	256 (8.6 × 10^3); 289 (5.8 × 10^3); 404 (2.06 × 10^4)
9	314 (2.23 × 10^4); 379 (3.23 × 10^4; 440 (1.64 × 10^5); 449 (1.78 × 10^5); 560 (1.33 × 10^4); 630 (3.93 × 10^4)
12	422 (4.77 × 10^4); 524 (1.44 × 10^4); 624 (1.44 × 10^4)
11	305 (2.87 × 0^4); 427 (1.71 × 10^5); 447 (1.59 × 10^5); 574 (1.74 × 0^4); 630 (4.31 × 10^4)
$AuTdTBuP^+$	416 (2.57 × 10^5); 524 (1.26 × 10^4); 564 (shoulder)
ZnTdTBuP	423 (3.13 × 10^5); 550 (1.32 × 10^4); 590 (4.3 × 10^3)

[a] ZnTdTBuP: tetra(3,5-diterbutylphenyl) zinc(II). $AuTdTBuP^+$: tetra(3,5-diterbutylphenyl) porphyrin gold(III).

Table 2. Excited State Energies Determined from 0−0 Absorption and Fluorescence Band Maxima, Except for ^{3}AuP, Where the Energy Is Taken as the Phosphorescence Maximum at 77 K in 2-Methyltetrahydrofuran

	E_{00} (^{1}ZnP*)/eV	E_{00} (^{1}S*)/eV	E_{00} (^{3}AuP)/eV
11	1.92		1.66
5		2.67	

suggest the existence of noticeable electronic interactions between the units in the ground state. The attachment of the electron-rich quaterthiophene spacer to the gold porphyrin induces a broadening and a tailing of the Q bands. We tentatively attribute this extra absorbance to charge transfer transitions from the quaterthiophene to the gold porphyrin. This assumption is supported by the observation that this residual absorbance is absent in compound **9**, which only contains ZnP.

Excited-state energies (Table 2) used to calculate driving forces for charge separation were determined using the spectroscopic properties.

Electrochemistry. The redox potentials of the porphyrin units were determined by cyclic voltammetry in dichloromethane (Figure S2, Supporting Information), and the half-wave potentials recorded for the compounds are gathered in Table 3.

In the dyad, the first reduction occurs on the gold porphyrin, which is reported to be a metal-based process. Conversely, the second reduction, also assigned to the gold porphyrin, is known to be localized on the porphyrin π-macrocycle. The half-wave potential of this second reduction appears to be anodically shifted by about 200 mV in the dyad compared to the reference gold tetraarylporphyrin (AuP^+). This probably results from the stabilization of the

Table 3. Redox Potentials of the Compounds[a]

	ZnP^+/ZnP	S^+/S	$AuP^+/AuP^•$	$AuP^•/AuP^-$
5		0.94 V		
9	0.64 V	0.86 V		
12		0.96 V	−0.57 V	−1.04 V
11	0.64 V	0.89 V	−0.58 V	−1.04 V
$AuTdTBuP^+$			−0.68 V	−1.23 V
ZnTdTBuP	0.74 V			

[a] The electrochemistry was recorded in dichloromethane with 0.15 M Bu_4NPF_6 as the supporting electrolyte, and all of the potentials are reported versus the saturated calomel electrode (SCE). ZnTdTBuP: tetra(3,5-diterbutylphenyl) zinc(II). $AuTdTBuP^+$: tetra(3,5-diterbutylphenyl) porphyrin gold(III). S = bisethynylquaterthiophene.

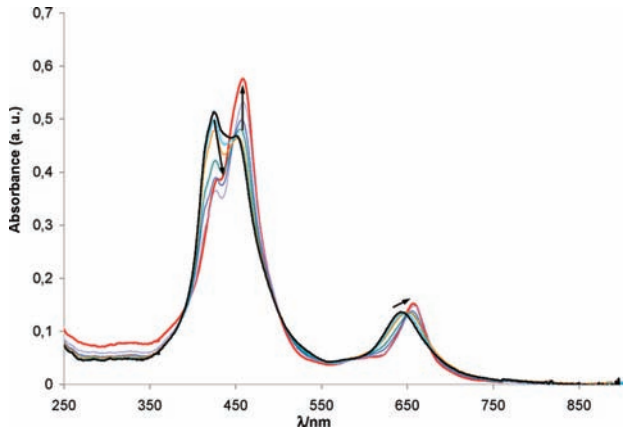

Figure 3. Spectra monitored in the course of the reduction of **11** in CH_2Cl_2 containing 0.15 M Bu_4NPF_6. The black bold trace is the initial spectrum, and the red bold trace is the final one. The arrows indicate the changes upon reduction.

π-molecular lowest unoccupied molecular orbitals (LUMOs), owing to their extension on the spacer. In the anodic region, the first oxidation is assigned to the formation of the radical cation on the zinc porphyrin. The lower oxidation potential of ZnP in **11** relative to the ZnTdTBuP is certainly due to the stabilization of the radical cation by the quaterthiophene spacer. Finally, the quaterthiophene oxidation is a reversible process since the spacer is substituted on both extremities. Importantly, the most oxidizable unit in the dyad is the zinc porphyrin moiety, which prevents the charge-separated state from decaying by a stepwise hole shift passing intermediately on the spacer.[14]

The electrochemical data confirm the existence of electronic interactions between the porphyrins and the spacer, deduced previously by the inspection of the electronic absorption spectra.

Spectroelectrochemistry. The dyad was investigated by spectroelectrochemistry to determine the exact absorption maxima of the reduced gold porphyrin and of the oxidized zinc porphyrin in this electronically coupled dyad. Indeed, due to the existence of substantial ground-state electronic interactions in this system, we could anticipate that the exact absorption spectra of these species could differ from those published in regular tetraaryl porphyrins. Figures 3 and 4 respectively show the UV−vis spectra of the radical of gold porphyrin and of the radical cation of the zinc porphyrin generated by the in situ electrolysis of dyad **11**. The oxidation of zinc porphyrin is accompanied by a strong bleaching of the Soret and Q bands of this porphyrin, whereas those of

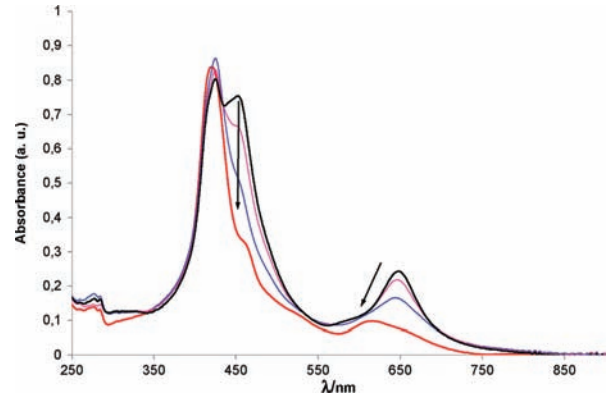

Figure 4. Spectra monitored in the course of the oxidation of **11** in CH_2Cl_2 containing 0.15 M Bu_4NPF_6. The black bold trace is the initial spectrum, and the red bold trace is the final one. The arrows indicate the changes upon oxidation.

the gold porphyrin remain quite stable, since the spectrum of the oxidized dyad shares some similarities with the spectrum of the reference AuP-S **12** (Figure 4).

Upon reduction of the gold porphyrin, the net absorption of the Soret region is less broad since one of the underlying bands is decreased in intensity (Figure 3). The Q-band region is also red-shifted to leave a spectrum that features some characteristics of the reference ZnP-S **9**.

Summarily, the oxidation of ZnP and the reduction of AuP^+ in the dyad induce changes that mostly occur in the Soret band region due to a decrease of the absorption of this transition, as already observed in tetraaryl porphyrins.

Fluorescence Spectroscopy. The steady-state fluorescence spectra of the dyad and the parent compound Spacer-ZnP **9** were recorded in toluene and dichloromethane and show that the singlet excited state is strongly quenched in both solvents (Figure S3, Supporting Information). Using time-correlated single-photon counting and streak camera measurements, the lifetime of the ZnP singlet in **11** was determined to be 70 ps in toluene, while that of the reference **9** is 1.8 ns. The lifetimes are in good agreement with the strong quenching observed in the steady-state experiments. Irradiation of the ZnP moiety in dichloromethane leads to rapid photodegradation in the dyad as well as the reference. Excitation of the AuP moiety leads to the formation of the nonemissive ^3AuP species within a few hundred femtoseconds, which precludes using emission to determine excited-state lifetimes.[27]

Femtosecond Transient Absorption Spectroscopy. Transient absorption spectroscopy was then undertaken to elucidate the deactivation processes occurring in the dyad. First, the transient absorption spectra of the references ZnP-S **9** and AuP-S **12** were recorded in toluene and dichloromethane (Figure S4, Supporting Information). Excitation of ZnP leads to the singlet excited state, which decays with a time constant of 1800 ps to form the characteristic spectral signature of the ZnP triplet. In CH_2Cl_2, the ZnP decomposes rapidly,

(26) Ljungdahl, T.; Pettersson, K.; Albinsson, B.; Mårtensson, J. *J. Org. Chem.* **2006**, *71*, 1677.
(27) Andréasson, J.; Kodis, G.; Lin, S.; Moore, A. L.; Moore, T. A.; Gust, D.; Martensson, J.; Albinsson, B. *Photochem. Photobiol.* **2002**, *76*, 47.

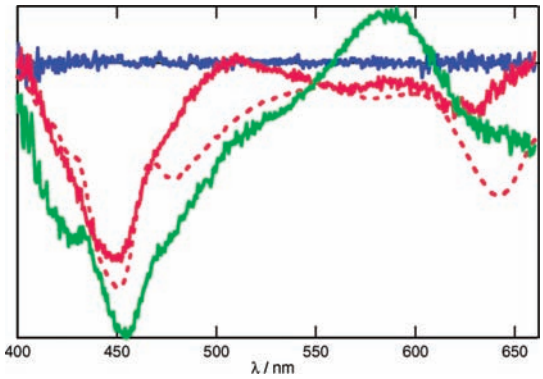

Figure 5. Transient absorption spectra recorded in toluene upon femtosecond excitation of the AuP moiety in dyad **11**. Blue = −10 ps; green = 40 ps; red = 2 ns. Dashed line: sum of difference spectra for the electrochemical reduction of AuP-S and oxidation of ZnP-S. The final spectrum of the photoproduct is similar to the expected spectrum for the CS product.

presumably undergoing electron transfer with the solvent. For **12**, the situation is more interesting. Despite the fact that oxidation of the bridge by ^{3}AuP is thermodynamically possible, we observed no indication of formation of AuP$^\bullet$ and S$^+$ radicals, either in toluene or in dichloromethane. Instead, the AuP$^+$ triplet decays back to the ground state without undergoing any photochemistry, with a lifetime of 2.4 ns in toluene and 500 ns in dichloromethane. Energy transfer to form the triplet of quaterthiophene can be ruled out, first, because the level of a triplet of quaterthiophene (1.8 eV) is uphill from that of the gold porphyrin triplet excited state (1.6 eV). Second, the absorption spectrum of the triplet of quaterthiophene is long-lived (microsecond) and is sufficiently different from that of the gold porphyrin to be detectable during the transient absorption spectroscopy study, which was not the case.[28]

The spectroelectrochemistry allows us to construct the expected spectrum for the CS product by adding the reduction and oxidation difference spectra (dashed line trace in Figure 5). For the dyad in toluene, following ZnP excitation, we observe initially the same spectrum as for the reference **9** (Figure 6). However, this spectrum rapidly decays to form an intermediate species which we, on the basis of spectroelectrochemical measurements, identify as the **ZnP$^+$−S−AuP$^\bullet$** charge-separated state (Figure 5).

The electron transfer occurs with the same time constant as the fluorescence lifetime (70 ps), which is consistent with electron transfer. The charge-separated state then returns to the ground state with a time constant of 3.3 ns. A small amount of ^{3}ZnP is formed in the back reaction, as evidenced by a long-lived fraction of the ZnP triplet seen in the transient absorption spectra, but the overwhelming majority of the recombination occurs in the ground state.

Upon excitation of the gold porphyrin, the rapidly formed triplet[27] oxidizes the ZnP moiety through hole transfer (HT; Figure 7). The kinetics show that the red part of the Soret band, where ZnP dominates, is bleached with the same rate as the absorption goes less negative in the red edge of the

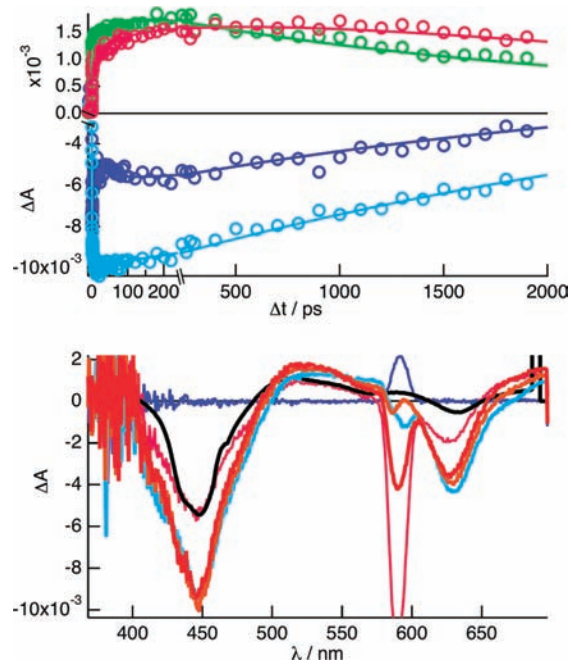

Figure 6. Transient spectra (bottom) and decays (top) of dyad **11** in toluene for ZnP excitation at 590 nm. (Top) Dark blue, 425 nm; light blue, 450 nm; green, 530 nm; red, 690 nm. (Bottom) Dark blue, −10 ps; light blue, 5 ps; orange, 50 ps; red, 250 ps; dark red, 2 ns. Black trace: ^{3}ZnP spectrum recorded for the ZnP-S reference compound **9** scaled to equal Soret band bleaching.

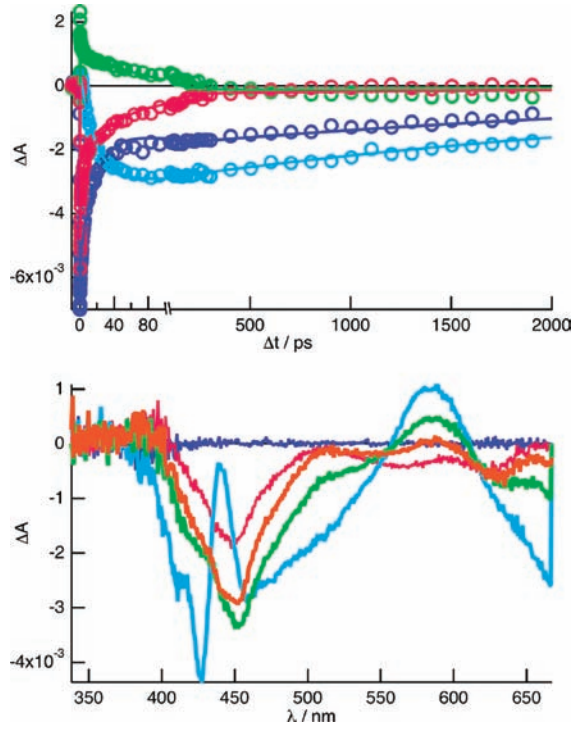

Figure 7. Transient spectra (bottom) and decays (top) of dyad **11** in toluene for AuP excitation at 690 nm. (Top) Dark blue, 430 nm; light blue, 440 nm; green, 580 nm; red, 660 nm. (Bottom) Dark blue, −10 ps; light blue, 5 ps; green, 70 ps; orange, 250 ps; red, 2 ns. The double peak in the Soret band is likely not associated with the CS process (see text).

spectrum, as we expect from spectroelectrochemistry. This process is slightly slower than the ET process, in line with its slightly lower driving force. Again, we would like to stress the fact that we see no sign of the oxidized bridge, despite

(28) Matsumoto, K.; Fujitsuka, M.; Sato, T.; Onodera, S.; Ito, O. *J. Phys. Chem. B* **2000**, *104*, 11632.

Table 4. Time Constants of Photophysical Processes in ps[a]

	toluene			CH_2Cl_2		
	k_{ET}	k_{HT}	k_{CR}	k_{ET}	k_{HT}	k_{CR}
11	70 ± 5	140 ± 10	3300 ± 100	*b*	20 ± 3	100 ± 10
13[c]	7	130*	130	2	*b*	90
14[c]	8	130*	240	2	2	170

[a] *Energy transfer process. k_{ET} = Electron transfer rate from singlet ZnP* to AuP^+. k_{HT} = Hole transfer rate from triplet AuP* to ZnP. k_{CR} = Rate of charge recombination reaction. [b] Rate not measurable. [c] From ref 4.

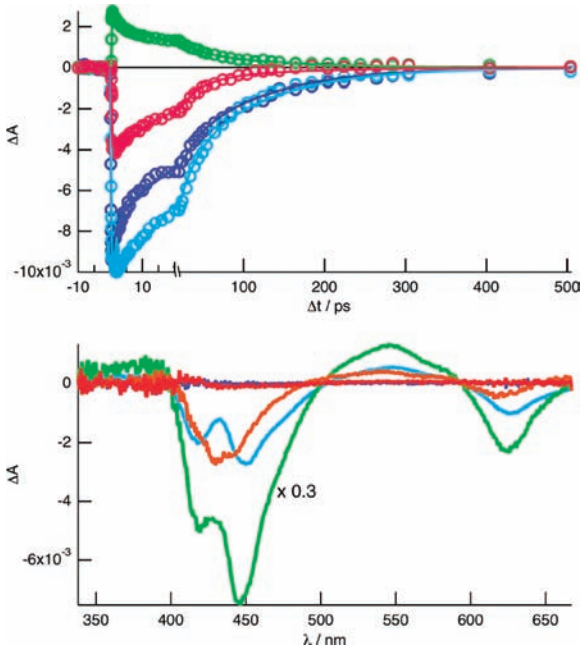

Figure 8. Transient spectra of dyad **11** in dichloromethane for AuP excitation at 690 nm. (Top) Dark blue, 420 nm; light blue, 450 nm; green, 545 nm; red, 630 nm. (Bottom) Dark blue, −10 ps; light blue, 5 ps; green; 20 ps; orange, 100 ps; red, 2000 ps. The double-peak feature in the Soret band disappears within about 10 ps and is likely not related to the charge-shift process (see text). Note that the 5 ps spectrum has been scaled by a factor of 0.3.

the favorable thermodynamics. The back charge shift occurs with the same rate as in the ET pathway (3.3 ns), something that is commonly observed in zinc/gold porphyrin dyads.[15,16] Just as for ET, recombination occurs in the ground state. We cannot monitor the complete decay to the ground state with the femtosecond laser, but the spectrum and lifetime of the CS intermediate is clearly different from that of ^{3}ZnP-S and ^{3}AuP-S references. Besides, supporting this conclusion is the observation that the ZnP Soret band bleach of **11** in toluene upon ZnP excitation measured by nanosecond flash photolysis is within the response function of the instrument (≈10 ns), in clear contrast to the ZnP-S reference (Figure S5, Supporting Information).

In the more polar solvent dichloromethane, the rates for both forward and backward CS are increased (Table 4 and Figure 8). Charge separation through hole transfer occurs with a time constant of 20 ps, while recombination occurs in the ground state with a time constant of 100 ps. These differences in rates certainly reflect that the energetics of the charge-transfer reaction differ in these two solvents, although they are difficult to estimate from the continuum dielectric model. We suspect that there is a different degree of ion pairing with the gold porphyrin according to the solvent polarity. In a polar solvent, such as dichloromethane, the counteranion is certainly partly or fully dissociated from AuP^+; therefore, the photoinduced reaction can be considered as a real hole shift. In toluene, the PF_6^- is certainly strongly associated with the AuP^+, and the reaction could be rather viewed as an electron transfer. It is also noteworthy that the ratio of forward to back charge transfer is lower in polar solvents than in nonpolar toluene.

Table 5. Driving Forces for Photoinduced Charge Separation in Dyad **11**

	$-\Delta G°_{ET}$/ eV	$-\Delta G°_{HT}$ (^{3}AuP/ZnP)/ eV	$-\Delta G°_{HT}$ (^{3}AuP/S)/ eV	$-\Delta G°_{CR}$ (^{3}AuP/ZnP)/ eV
11	0.70	0.44	0.19	1.22

In addition to the formation of the charge-shifted state, we observe ultrafast relaxation upon AuP excitation in the dyad in both solvents. The initial spectrum is characterized by a double peak in the Soret band bleach. This feature disappears on a 10−20 ps time scale to be replaced by the ^{3}AuP signature, which then converts into the spectrum of the charge-shifted species. The origin of this relaxation process is unknown, but we think it is likely related to relaxation of the ZnP−S−AuP* state, where the electronic communication between D, S, and A is changed in the excited state and may also be related to the ground-state charge transfer we observe.

The excitation of ZnP in **11** is not as selective as for AuP^+ excitation, and some ^{3}AuP is formed in addition to the ^{1}ZnP initially. Although, the formation of an intermediate charge-shifted state is clearly resolvable in the kinetic analysis. For comparison, the ^{3}ZnP spectrum (black trace in Figure 6) recorded for ZnP-S reference **9** is included. We can notice the difference between the ^{3}ZnP spectrum and that of the CS intermediate.

Discussion

The emission data and the redox potentials were used to build an energy diagram of the different states of interest of dyad **11** (Scheme 3). From the energies, we conclude that electron transfer from the zinc porphyrin singlet excited state to the gold porphyrin and hole transfer from gold porphyrin triplet excited state to the quaterthiophene or to the zinc porphyrin are all exergonic processes (Table 5). If the solvations of the zinc and the gold porphyrin radical cation are similar, we can consider that the free energies for charge separation are independent of the solvent polarity,[18] since the Columbic terms are zero for a charge shift reaction. From the redox potentials, we can estimate the position of $\mathbf{ZnP^+-S^--AuP^+}$. This state lies 0.5 eV above the singlet excited state of ZnP*; therefore, a forward electron transfer via a hopping mechanism is unlikely from ZnP*. On the other hand, the hole transfer from the triplet excited state of AuP^+ to the quaterthiophene spacer is an exergonic reaction, but we have not detected the formation of $\mathbf{X-S^+-AuP^\bullet}$ by transient absorption spectroscopy either in dyad **11** or in the reference compound **12**. We are not certain at this point why the hole transfer does not take place, but it is entirely clear from the transient spectroscopy that the charge-separation

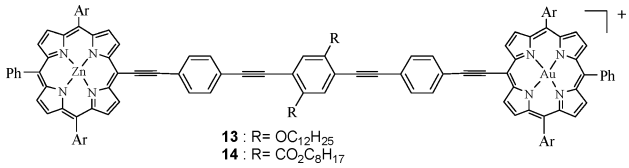

Figure 9. Structures of the dyads **13** and **14**.

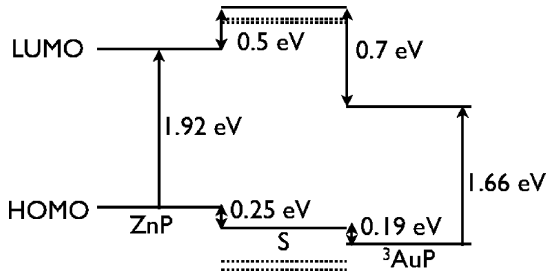

Figure 10. Orbital energies calculated from electrochemical potentials and excited-state energies. Dashed lines: HOMO and LUMO of the OPE spacers in **13** and **14**. Straight lines: HOMO and LUMO of the quaterthiophene in **11**.

reactions in dyad **11** essentially occur according to a superexchange mechanism and that the hole never resides on the bridge.

The rate of formation and the lifetime of the charge-shifted state is strongly solvent-dependent, as we have also observed for ZnP−AuP dyads **13** and **14** linked by OPE spacers (Table 4 and Figure 9). Similarly, we also observe virtually no difference in the lifetime of the CS state formed via hole transfer and that formed via electron transfer. Our explanation for the behavior in the present dyad **11** is similar to that given for the OPE dyads, namely, that the heavy gold atom blurs the spin identity of the CS state.[4]

Given that the chromophores are identical, and the D−A distances in **11**, **13**, and **14** are very similar, we can compare the photophysical behavior of the new dyad **11** with those of the previously studied dyads **13** and **14** (Figure 9 and Table 4).[4]

Figure 10 shows the orbital energy diagram of the dyads **11**, **13**, and **14** calculated from spectroscopic and electrochemical data. In comparison with the OPE bridges in dyads **13** and **14**, the highest occupied molecular orbital (HOMO) of the quaterthiophene bridge lies just between that of ZnP and that of the AuP^+ HOMO, while the energy gap between the LUMO of ZnP and that of quaterthiophene is a bit larger than that of the OPE bridges (Figure 10). Thus, one would expect a faster rate for the hole transfer reaction upon AuP^+ excitation and a slower rate of electron transfer upon ZnP excitation in **11** versus those in **13** and **14**. Indeed, with the quaterthiophene bridge, we get hole transfer in both CH_2Cl_2 and toluene instead of triplet energy transfer (CH_2Cl_2) or no reaction (toluene) observed for the OPE bridges in dyads **13** and **14**. The stronger hole transfer coupling expected from the closer-lying HOMOs thus favors HT over triplet energy transfer in **11**. Conversely, the electron transfer rate measured in toluene with **11** is slower than in dyads **13** and **14**. Superexchange by electron transfer is unlikely in the case of AuP^+ excitation, due to the large energy spacing between the LUMO of the AuP^+ and that of the quaterthiophene (Figure 10). Indeed, according to the superexchange theory, the electron transfer rate is inversely proportional to the energy difference between these two levels.[1,11]

The bisethynyl quaterthiophene modifies significantly the rates and the nature of the deactivation processes occurring upon excitation of the zinc or gold porphyrin. First, in toluene, the latter spacer affords an almost quantitative charge separation yield irrespective of which porphyrin is photoexcited, whereas in dyads **13** or **14**, excitation of AuP^+ is accompanied by energy transfer to form the ZnP triplet state (Table 3). Another valuable distinction of the bisethynyl quaterthiophene is that the charge-separated state recombines with the ground state instead of ^{3}ZnP, as observed in **13** or **14** in toluene. This is certainly a consequence of the lower-lying charge shifted state in the new dyad **11**, owing to the lower oxidation potential of the ZnP unit. As a result, the triplet excited state of ZnP might be located slightly above that of $\mathbf{ZnP^+-S-AuP^\bullet}$ even in toluene. Most importantly, dyad **11** gives the longest-lived charge-separated state and the largest k_{CS}/k_{CR} ratio in toluene. This is consistent with a charge recombination leading directly to the ground state, instead of to the triplet state of ZnP for **13** and **14**. As a consequence, the driving force of this process is larger and pushes it further away in the inverted Marcus region, hence resulting in a slower rate.[1,11]

Conclusion

We have described the synthesis of a novel bis porphyrin dyad performing a very fast single-step photoinduced electron transfer over a long distance via a bridge-mediated superexchange mechanism. This new dyad shows that the attachment directly on the meso position of a π-conjugated bridge via an ethynyl linker is a well-suited strategy to perform efficient and long-range photoinduced charge separation between two distant porphyrins. Furthermore, the bisethynyl quaterthiophene is a better suited spacer than oligophenyleneethylenes, because it promotes charge separation over energy transfer, it prohibits the decay of the charge-separated state to the ZnP triplet state, and finally it permits reaching a longer-lived charge-separated state. It also belongs to the rare cases in which photoinduced charge separation can be brought about by excitation of any of the sensitizers of a bichromophoric dyad.[16] This new dyad represents, therefore, an attractive photochemical system to build more complex systems for solar energy conversion or molecular electronic applications.

Acknowledgment. The French Research Ministry is gratefully acknowledged for the financial support of these researches through the programs "ACI Jeune Chercheur" and the ANR blanc "PhotoCumElec" and the European Community for COST D35 program.

Supporting Information Available: ^{1}H NMR of the new compounds and extra physical charaterizations. This material is available free of charge via the Internet at http://pubs.acs.org.

IC800727E